ECI Symposium Series, Volume RP5: Proceedings of 7th International Conference on Heat Exchanger Fouling and Cleaning - Challenges and Opportunities, Editors Hans Müller-Steinhagen, M. Reza Malayeri, and A. Paul Watkinson, Engineering Conferences International, Tomar, Portugal, July 1 - 6, 2007

EXPERIMENTS AND MODELLING OF CALCIUM SULPHATE PRECIPITATION UNDER SENSIBLE HEATING CONDITIONS: INITIAL FOULING AND BULK PRECIPITATION RATE STUDIES

F. Fahiminia[1,2], A. P. Watkinson[1] and N. Epstein[1]

1. Department of Chemical and Biological Engineering, The University of British Columbia, 2360 East Mall, Vancouver, B.C., Canada V6T 1Z3
2. Present Address: NOVA Research and Technology Centre, NOVA Chemicals Inc., 2928-16 Street NE, Calgary, Alberta, Canada T2E 7K7

ABSTRACT

Crystallization of calcium sulphate, an inverse solubility salt, on a heated surface under sensible heating conditions has been studied. A temperature measurement technique was employed to detect initial fouling rates. Fouling experiments were carried out to determine how process variables such as surface temperature and velocity affect the initial fouling rates of calcium sulphate scaling. Experimental results show that, at a given surface temperature, there exists a maximum initial fouling rate for a range of fluid velocities. Also, this maximum rate and the fluid velocity at which it occurs both increase as the surface temperature increases. These observations are all qualitatively in agreement with the Initial Fouling Rate Model (IFRM) of Epstein (1994). The fouling experiments were supplemented by kinetic batch experiments to make a comparison between fouling activation energies and purely chemical activation energies.

INTRODUCTION

The deposition of calcium sulphate on heat transfer surfaces is a frequently encountered problem when dealing with boiler feedwater, cooling water undergoing an appreciable temperature rise, and seawater more generally. It can cause a decline in operating efficiency of power plants, food processing works, pulp mills and other chemical industries. The principal mode of calcium sulphate deposition is variously referred to as crystallization fouling, precipitation fouling or scaling. This mode may at times be accompanied by some particulate fouling of suspended calcium sulphate, which the present study made a special effort to eliminate or at least minimize.

One motivation for the present study is the fact that previous investigations of $CaSO_4$ scaling from aqueous solutions undergoing sensible heating reported differing effects on the fouling rate of varying the fluid velocity. While the majority of studies (e.g. Bansal and Müller-Steinhagen, 1993; Mori et al, 1996; Bohnet et al., 1999 Middis et all, 1998) have shown a decline in the initial fouling rate, $\dot{R}_{fo}$, with increasing fluid velocity, V, at least two (Ritter, 1983; Najibi et al., 1997) have shown an increase of $\dot{R}_{fo}$ with V, and one (Mwaba et al., 2001) concluded that "deposition is independent of velocity". This conclusion was actually based on values of fouling rates at three velocities (0.3, 0.6 and 1.0 m/s) that showed a maximum at the intermediate velocity, albeit a flat one. Such a maximum is quite suggestive of the Initial Fouling Rate Model that relates deposit attachment to a surface to fluid residence time at the surface (Epstein, 1994) and that we have gainfully applied to both chemical reaction fouling (Epstein, 1994; Wilson and Watkinson, 1996; Rose et al., 2000, 2001) and colloidal particle deposition under attractive electrical-double-layer conditions (Vašák et al., 1995). This model, which incorporates both velocity and surface temperature effects, was therefore expressed in terms appropriate to crystallization fouling and applied to measurements of the initial calcium sulphate fouling rates.

INITIAL FOULING RATE MODEL (IFRM)

Consider precipitation fouling from a solution in well developed turbulent flow parallel to a heat transfer surface. In the case of an inverse solubility salt such as gypsum ($CaSO_4 \cdot 2H_2O$) above 45°C, precipitation occurs due to the difference between the bulk concentration C_b of the solution, which is supersaturated with respect to the surface temperature T_s, and the saturation concentration C_s at T_s.

The mass transfer flux of solution to the vicinity of the surface or wall is given by

$$\phi = k_m (C_b - C_w) \qquad (1)$$

where C_w is the concentration of the precipitating solute in the solution adjacent to the wall. Attachment to the wall occurs by surface integration at saturation conditions, given by

$$\phi = k_a \left(C_w - C_s\right)^n \tag{2}$$

where n is the order of the surface reaction. Combining Equations (1) and (2),

$$\phi = \frac{\Delta C}{\frac{1}{k_m} + \frac{1}{k_a^{1/n}} \phi^{(n-1)/n}} \tag{3}$$

where $\Delta C = (C_b - C_w) + (C_w - C_s) = C_b - C_s$. Assuming, after Konak (1974) and many others, that n = 2 for precipitation fouling of calcium sulphate, then on rearranging and squaring Equation (3) we arrive at

$$\frac{\phi^2}{k_m^2} - \left(\frac{2\Delta C}{k_m} + \frac{1}{k_a}\right)\phi + \left(\Delta C\right)^2 = 0 \tag{4}$$

Given that $\phi < k_m \Delta C$, the solution to the quadratic Equation (4) is

$$\phi = k_m \left(\frac{k_m}{2k_a} + \Delta C - \sqrt{\frac{1}{4}\left(\frac{k_m}{k_a}\right)^2 + \frac{k_m}{k_a}\Delta C} \right) \tag{5}$$

Equation (5) has been previously derived by Krause (1993) and others.

The mass transfer coefficient k_m is in general given by

$$k_m = \nu_* / k' Sc^{2/3} \tag{6}$$

where k' is a dimensionless constant, while the attachment coefficient k_a has commonly been taken as a conventional rate constant k_r that bears the usual Arrhenius relationship to the surface temperature. What distinguishes the present Initial Fouling Rate Model from other models is that k_a is here written as (Epstein, 1994)

$$k_a \propto k_r \upsilon / \nu_*^2 = \upsilon e^{-\Delta E / RT_s} / k'' \nu_*^2 \tag{7}$$

where k'' is a dimensional coefficient that includes the Arrhenius pre-exponential factor. The term υ / ν_*^2, which has the dimensions of time, is inversely proportional to the fluid velocity within the viscous sublayer and directly proportional to the shedding period of that sublayer. It thus varies as the fluid residence time near the wall and incorporates the idea that the longer the fouling material spends at the heat transfer surface, the greater the probability that it will adhere to that surface. The deposition flux ϕ is related to the initial fouling rate $\dot{R}_{fo}$ by

$$\dot{R}_{fo} = \frac{\phi}{\lambda_f \rho_f} \tag{8}$$

so that on combining this equation with Equation (5) the result is

$$\dot{R}_{fo} = \frac{k_m}{\rho_f \lambda_f} \left(\Delta C + \frac{k_m}{2k_a} - \sqrt{\frac{1}{4}\left(\frac{k_m}{k_a}\right)^2 + \frac{k_m}{k_a}\Delta C} \right) \tag{9}$$

Knowing in full all the relevant fluid and deposit properties at the temperatures involved, as well as the concentration driving force ΔC, fluid bulk velocity V and pipe diameter d, Equation (9), in conjunction with Equations (6) and (7), models the initial fouling rate with three adjustable parameters, k', k'' and ΔE. Like the more conventional models, it shows $\dot{R}_{fo}$ increasing as surface temperature increases for any given velocity and fixed ΔC, but unlike other models, it shows an increase of $\dot{R}_{fo}$ with velocity to a maximum and then a decrease at any given surface temperature, and it shows the velocity at which this maximum occurs as increasing with surface temperature, again all at fixed ΔC.

EXPERIMENTAL

The apparatus, Figure 1, employed in fouling experiments, consisted of a flow loop in which the calcium sulphate solution was continuously recirculated from a holding tank through a 1-μm filter, the heated test section, a series of double pipe coolers and back to the holding tank. The test section was constructed of a drawn T304 stainless steel (ASTM A269-80A) tube with a length of 1.83 m, an outside diameter of 9.525 mm, a wall thickness of 0.254 mm and a heated length of 0.771 m, which is subjected to electrical resistance heating at a

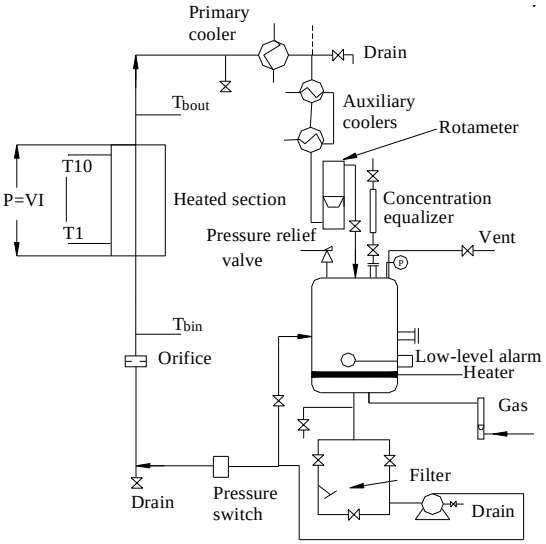

Figure 1: Schematic of the Tube Fouling Unit, after Wilson (1994)

constant and uniform heat flux. Bulk inlet and outlet temperatures were measured by thermocouples. The bulk inlet temperature was maintained constant during each experiment (at 51˚C for all of the experiments), while clean tube surface temperatures were varied from 66 to 87˚C, as measured by ten thermocouples spaced longitudinally on the outside of the vertical tube. The rate of rise in surface temperature gave a measure of the local fouling resistance at that temperature. This Tube Fouling Unit (TFU) (Wilson and Watkinson, 1996; Rose et al., 2000) was configured such that test sections were used only once, and then sectioned to allow in situ deposit examination and further analysis of the nature of the deposit material, either by optical microscopy, scanning electron microscopy, elemental analysis or deposit coverage studies. A concentration equalizer (installed on top of the holding tank) was employed to keep concentration constant during each experiment. It was isolated from the rest of the apparatus, which is running at high pressure during the experiment, using a connective valve and then, after adding the required chemicals to the equalizer, the valve was opened gradually to let chemicals flow into the holding tank while the pressure is kept constant.

Due to the longitudinal temperature gradient at the surface of the tube, the highest rates of fouling occurred at the locations of the highest temperature thermocouples, and thus limited the duration of an experiment. Because clean surface temperatures were as high as 87˚C, it was necessary to maintain some over-pressure (typically about 100 psig) on the test section to prevent the onset of boiling as the wall temperature rose due to fouling. Because of the high temperature limitation, some of the thermocouples from the low temperature regions of the tube gave barely measurable fouling rates. Reynolds numbers based on local fluid properties were varied from 2100 to 36000 to provide adequate data for a study of the velocity effect on the initial fouling rates.

Batches of calcium sulphate solution, about 65 liters, were prepared by dissolving calcium nitrate, $Ca(NO_3)_2 \cdot 4H_2O$ (Fisher Scientific, Industrial Grade 99%), and sodium sulphate, Na_2SO_4 (Fisher Scientific, Industrial Grade 99%), in deionised water. After ensuring the required concentration level by using EDTA titration, the solution was added to the holding tank. Prior to the addition of heat to the test section, the solution was circulated for one hour to ensure a thoroughly well mixed chemical system. The power to the test section was then applied to achieve the operating conditions required. Heating up the test section to steady state took approximately 30 minutes.

Kinetic studies of calcium sulphate precipitation were carried out using a Jacketed Glass Reactor (JGR). It was constructed from glass with a working volume of 0.7 liter and a diameter of 10 cm. A magnetic stirrer, under constant stirring rate, was used to keep the temperature and concentration uniform throughout the reactor. The JGR was employed for performing batch experiments, in which the same solutions were used as for the TFU experiments. The bulk temperature was varied in the range of 60 to 84˚C, while the initial concentrations of $CaSO_4$ were 3100 and 3400 ppm by weight.

FOULING EXPERIMENTAL RESULTS

Fouling in the loop experiments was detected thermally. The local heat transfer coefficient at a given thermocouple location along the length of the test section was determined from the following equation, where $\dot{q}$ was evaluated from the voltage and current applied to the test section, T_b from the bulk inlet and outlet fluid temperatures and T_w calculated from the measured thermocouple temperature, $T_{w,o}$, by solution of the steady state conduction equation with internal heat generation:

$$U = \frac{\dot{q}}{(T_w - T_b)} \tag{10}$$

The fouling resistance R_f was determined from

$$R_f = U^{-1} - U_c^{-1} \tag{11}$$

and the initial fouling rate from

$$\dot{R}_{fo} = dR_f / dt\big|_{t=0} = d\left(U^{-1}\right)/dt \tag{12}$$

The flow rate and hence velocity of the fluid through the TFU was measured using a calibrated rotameter. The reported bulk velocity is the time averaged value over the duration of the experiment at any given level.

For each experiment, the thermal fouling results were measured from up to 10 thermocouples located at various axial positions. For all of the experiments, the thermocouples showed a linear increase in wall temperature with time after the occurrence of two consecutive events, i.e. a delay time and a roughness control period. This made the analysis for the initial fouling rate straightforward. In the region where the temperature is increasing at a constant rate, the corresponding plot of reciprocal heat transfer coefficient versus time is linearly regressed and from Equation (12) the slope was assumed equal to the initial fouling rate in the absence of the roughness effect, i.e. at time zero immediately after the delay period.

Figure 2 illustrates a complete view of the fouling progress stages observed for one thermocouple (x = 715 mm for TFU 703). It consists of four different regions: a short heat-up time (about half an hour), a nucleation delay time (horizontal region), a roughness control period in which the heat transfer enhancement of the scale roughness over-rides the heat transfer resistance of the scale, and a final region in which scale resistance

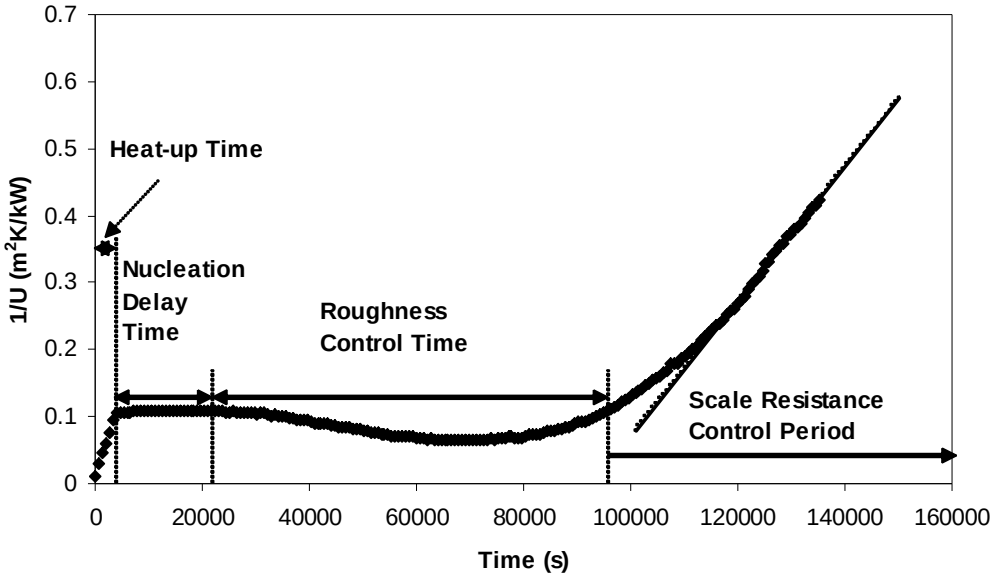

Figure 2: Different Fouling Stages at x = 715 mm for TFU 703 (V = 1.2 m/s, C_b = 3128ppm)

over-rides scale roughness.

Combining Equations (8) and (3) with n=1, i.e. assuming for illustration purposes a first order reaction, and anticipating the type of fouling Arrhenius plots described below, the IFRM in its simplest form becomes:

$$\dot{R}_{fo} = \frac{\Delta C}{\frac{1}{\alpha V} + \frac{V^2}{\beta e^{(\frac{-\Delta E}{RT_{w,c}})}}} = Ae^{-\Delta E_f / RT_{w,c}} \qquad (13)$$

In Equation (13), two different activation energies are recognized: ΔE, the purely chemical activation energy, and ΔE_f, the fouling activation energy that characterizes the entire fouling process at a given velocity. For small fluid velocities, i.e. when mass transfer controls, fouling activation energy ΔE_f must approach a small value. But for high fluid velocities, i.e. when surface attachment controls, the fouling activation energy approaches the purely chemical activation energy.

The initial fouling rate measurements allowed us to investigate the aforementioned features of the model. For instance, Figure 3 shows a fouling Arrhenius plot $(\ln \dot{R}_{fo} = \ln A - \Delta E_f / RT_{w,c})$ for a given experiment, where individual thermocouple results were utilized to determine the surface temperature at a velocity of 1.2 m/s. The fouling activation energy ΔE_f for this experiment was determined as 387 kJ/mol. The results for all runs performed at a concentration of 3400 ppm (wt.) are presented in Table 1.

From Table 1, a kinetic compensation effect is evident where both the fouling activation energy, ΔE_f, and the pre-exponential term, A, increase with velocity. The increase in ΔE_f with velocity is consistent with the

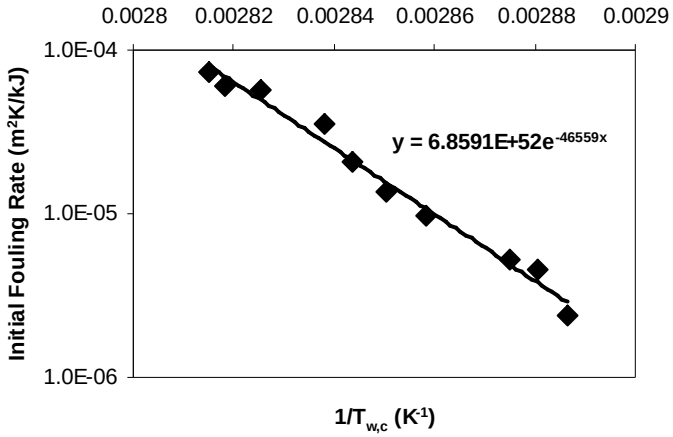

Figure 3: Arrhenius plot for TFU 809 (V=1.2 m/s)

mathematical model. From Table 1, it is possible to use the Arrhenius expression to determine initial fouling rate at a given value of $T_{w,c}$ for each experiment and hence investigate the effect of velocity on the initial fouling rate. Thus Figure 4 shows the calculated results at six different surface temperatures where the initial fouling rate is dependent upon the velocity. In all cases one can see the presence of a maximum deposition rate at a critical velocity as predicted by the model (Equation 9). Also, as the clean inside wall temperature decreases, the value of the maximum $\dot{R}_{fo}$ decreases, and the location of the maximum for the four highest temperatures shifts towards a decreasing velocity, both trends being consistent with the model. At a wall temperature of 83˚C it seems that the maximum initial fouling rate occurs around 1.2 m/s. At lower wall temperatures, below 73˚C, there is a smaller distinction between initial fouling rates at different velocities, with experimental scatter probably playing a more significant role.

Table 1: Arrhenius parameters for Calcium Sulphate Fouling Experiments (C = 3400 ppm)

Run No.	$T_{w,c}$ (°C)	T_b (°C)	V (m/s)	$Re(T_{f,avg})$	ΔC (kg/m^3)	ΔE_f (kJ/mol)	A (m^{2}K/kJ))
812	71-87	51-62	0.1	2200	0.91-1.20	66	7.49E+4
811	66-83	51-61	0.2	4200	0.84-1.14	159	8.22E+18
817	71-83	51-62	0.3	6200	0.92-1.13	170	5.15E+20
804	72-83	51-63	0.5	10600	0.94-1.12	268	1.65E+35
803	72-83	51-63	0.7	14700	0.95-1.12	304	3.62E+40
806	72-83	51-62	1.0	20800	0.94-1.12	367	7.64E+49
809	73-82	51-62	1.2	25100	0.96-1.11	387	6.86E+52
807	73-83	51-62	1.4	29400	0.96-1.13	425	1.65E+58
808	73-83	51-62	1.6	33800	0.97-1.12	514	1.80E+71

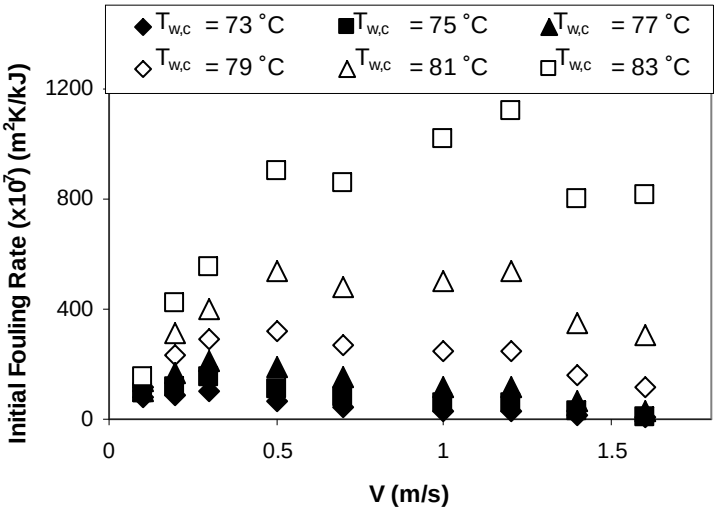

Figure 4: Effect of Velocity on Initial Fouling Rate (C = 3400 ppm)

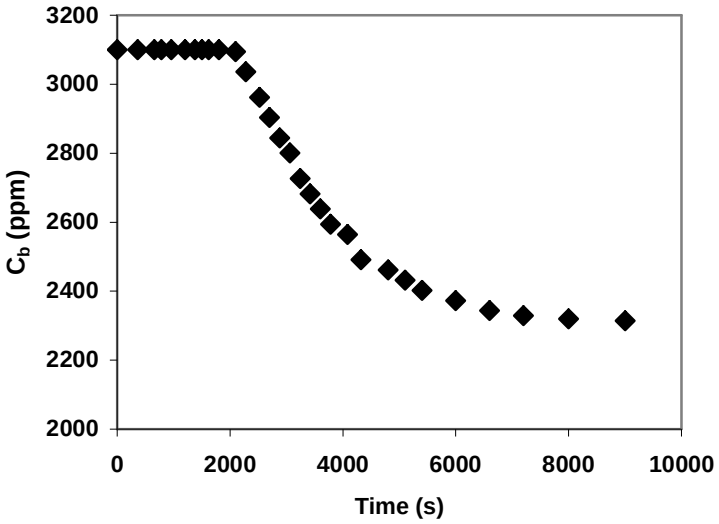

Figure 5: Plot of Calcium Sulphate Concentration vs. time (T_b = 80˚C, C_{b0} = 3100 ppm)

KINETIC RESULTS

In order to separate the contribution of surface reaction (integration) from that of mass transfer, purely chemical activation energy values were generated through kinetic studies of calcium sulphate precipitation in the Jacketed Glass Reactor (JGR). For all the experiments the stirring rate was kept constant at its highest value of 300 revolutions/minute, to assure a uniform temperature and concentration throughout the reactor, and hence surface integration control. During each experiment calcium sulphate concentration was measured and recorded with time using a conductance meter (Jen Way 4042). Figure 5 illustrates calcium sulphate concentration variation with time at T_b = 80˚C and C_{b0} = 3100 ppm. A proper rate equation was needed to interpret the trend observed in Figure 5. Although several expressions have been proposed for kinetics of calcium sulphate crystallization, Smith and Sweett (1971) suggested that the following equation, given by Nancollas (1968) and Konak (1974), describes calcium sulphate precipitation best:

$$-\frac{dC_b}{dt} = k_R A_c (C_b - C_s)^2 \qquad (14)$$

In contrast to Bansal et al. (2005), who lumped k_r and A_c together as a single constant despite the fact that A_c increases during the course of a crystal growth experiment, the approach adopted here was that of O'Rourke and Johnson (1955). In their method, which is applicable to cases where the surface area of the crystal changes significantly with time but the shape of the growing crystals remain invariant during the growth process, crystal surface area is given by:

$$A_c = A_{co}(m/m_\circ)^{2/3} \quad (15)$$

where A_c is the surface area of crystals at any time t, A_{co} and m_o are the surface area and the mass of crystals at time t_o, and m is the mass of crystals at time t. From Equation (15), the term A_c as a function of solute concentration rather than of crystal mass becomes

$$A_c = A_{c1}\left(\frac{C_{bo} - C_b}{C_{bo} - C_{b1}}\right)^{2/3} \quad (16)$$

where C_{bo} is the initial bulk concentration (at the start of the experiment), C_{b1} is the first concentration measurement after precipitation has started, A_{c1} is the total surface area of crystals corresponding to concentration C_{b1}, and C_b is the concentration at any time t. Therefore it was possible to incorporate Equation (16) with any proper kinetic model proposed by other researchers. For instance, combining Equations (14) and (16), we arrive at the following differential equation:

$$-\frac{dC_b}{dt} = k_R A_{c1}\left(\frac{C_{bo} - C_b}{C_{bo} - C_{b1}}\right)^{2/3}(C_b - C_s)^2 \quad (17)$$

the integral form from time t_1 being

$$-\int_{C_{b1}}^{C_b} \frac{dC_b}{\left(\frac{C_{bo} - C_b}{C_{bo} - C_{b1}}\right)^{2/3}(C_b - C_s)^2} = k(t - t_1) \quad (18)$$

where $k = k_R A_{c1}$.

For all the performed experiments, Equation (18) was numerically integrated using an adaptive Simpson quadrature technique and the results were plotted vs. time to evaluate k. Figure 6 shows a typical plot for a bulk temperature of 65˚C and the initial concentration of 3400 ppm. It introduces a unique reaction rate constant which was determined as 401 $(gmol/l)^{-1}.s^{-1}$. This method was employed for other batch experiments to extract reaction rate constant values corresponding to each temperature and then a pure chemical activation energy was evaluated. This procedure generated values of 254 and 210 kJ/mol for initial concentrations of 3100 and 3400 ppm, respectively.

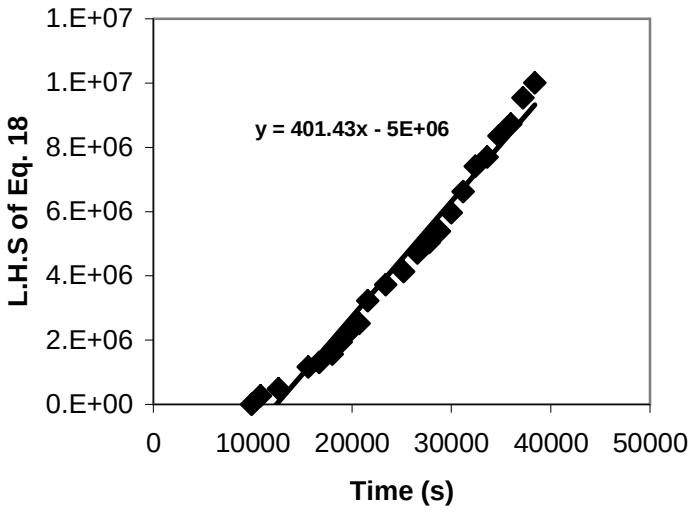

Figure 6: Reaction Rate Constant Evaluation Based on Equation (18) (T_b = 65˚C, C_{b0} = 3400 ppm)

MODELLING AND DISCUSSIONS

To explore the applicability of the Initial Fouling Rate Model, Equation (9), the fouling experimental results were employed. The ranges of temperatures and other conditions covered for each of the nine runs is recorded in Table 1.

Of the 9 x 10 = 90 sets of readings made in the nine runs performed, there were six sets when thermocouples at or near the bottom of the heated section showed no temperature increase, i.e. no fouling controlled by the thermal resistance of the scale throughout the entire course of the run, which left 84 data points with which to test the IFRM quantitatively. In doing so, all fluid properties associated with the mass transfer coefficient were based on the film temperature $(T_b + T_s)/2$, and those in the attachment terms were based on the deposit-fluid interface temperature T_s, assumed equal at all times to the clean inside wall temperature, $T_{w,c}$. Thus effects of roughness and blockage are ignored. In the expression for friction velocity $v_* = V(f/2)^{0.5}$, which occurs in both the mass transfer and attachment terms, the friction factor f was obtained from the Petukhov (1970) equation,

$$f = (1.58\ln \mathrm{Re} - 3.28)^{-2} \quad (19)$$

which applies to the transition and turbulent flow regimes for tubular flow. Solution viscosities were measured with an Ubbelohde viscometer and densities with specific gravity bottles over the temperature range 25-80°C. For evaluating Sc, molecular diffusivities of calcium sulphate in water solution reported by Bohnet (1987) over a small temperature range were extended to the desired temperatures by assuming constancy of $D\mu/T$, after Einstein (1905). Terms such as those rounded off to one or two significant figures in Table 1 were accurately determined to at least three significant figures and applied as input to the model at each thermocouple location, as were also the associated fluid properties and the friction velocity. The term $\rho_f \lambda_f$, which was taken as 2199 $kg.W/m^4.K$ (Fahiminia, 2007), and which functions only as a multiplier of both k' and k'' in the IFRM, will influence the best-fit values of k' and k'', but not how well the model fits the $\dot{R}_{fo}$ data. The temperature and velocity effects that characterize the IFRM depend

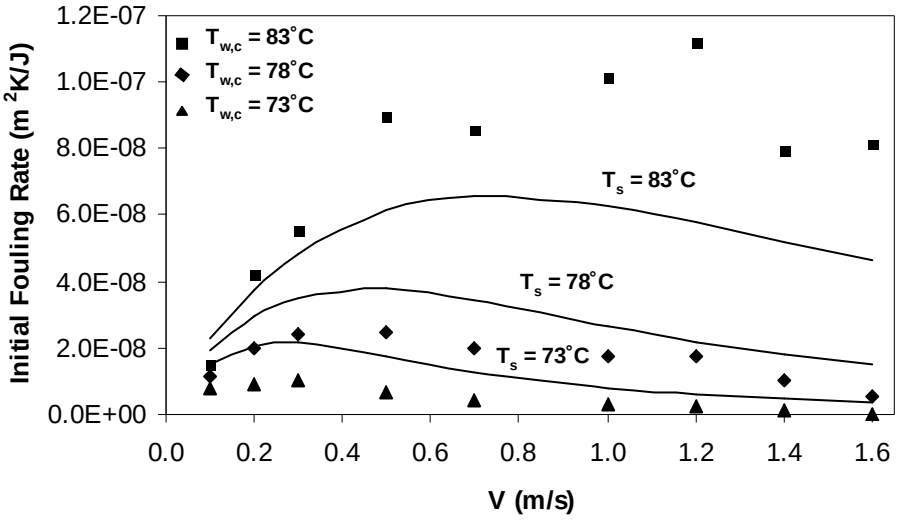

Figure 7: Comparison of Model Predictions to Experimental Data Obtained from the Arrhenius Type Equations

on constancy of $\Delta C(=C_b - C_s)$. In the present study, any increase in ΔC along the test section due to increases in T_s and corresponding decreases of C_s were relatively small (see Table 1).

The best fit of the IFRM was achieved by means of a non-linear least squares regression with respect to $\dot{R}_{fo}$ of the 84 data points, using the Levenberg-Marquardt method to perform the non-linear curve-fitting. The average absolute % deviation (AAD) between the data points and the best fit was 67.4% and the corresponding values of the adjustable parameters were $k' = 3.55$, k'' = 1.40 x 10^{-39} kg.s^2/m^4 and ΔE =263 kJ/mol. Figure 7 shows data, again from the Arrhenius fouling plots, compared with the model at three clean inside wall temperatures. Both data and model show the same qualitative trends described above, but the data fall consistently below the model lines for the two lower temperatures and consistently above for the higher. These deviations account for the sigmoidal pattern of the 84 experimental points in the parity plot of Figure 8. The fact that, as in the kinetic results, the value of 263 kJ/mol for the surface reaction activation energy, ΔE, predicted by the model is considerably smaller than the highest value of ΔE_f in Table 1, for which the surface reaction is most in control of the fouling processes, is another manifestation of disagreement between what the model has generated and what, on theoretical grounds, one would expect it to generate.

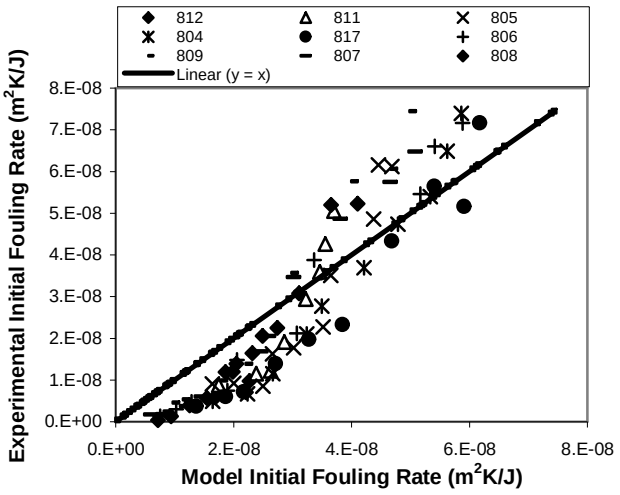

Figure 8: Comparing Experimental and Model Initial Fouling Rate Results

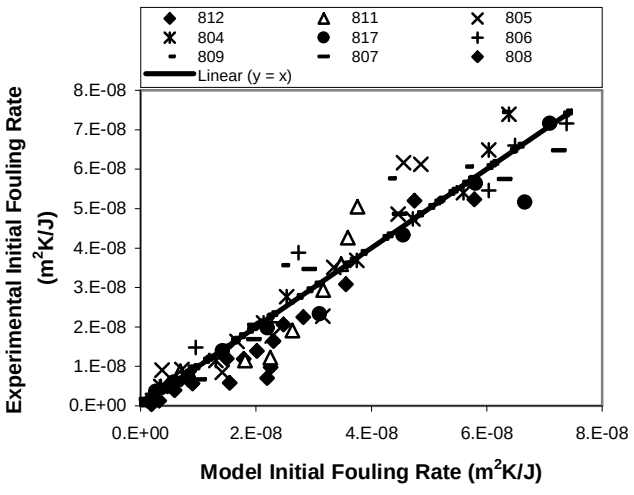

Figure 9: Comparing Experimental and Modified Model Initial Fouling Rate Results

Significant improvement of the IFRM curve-fit was obtained by introducing the multiplier aT_s^b into the denominator of the expression for k_a given by Equation (7). The rationale for this procedure is the assumption that crystal nucleation on the precipitation surface, which occurs simultaneously with crystal growth, is very temperature dependent and has been neglected in the original model, is thus crudely accounted for. The procedure adds one additional adjustable parameter, b, to the model, the coefficient a being lumped into the adjustable parameter k''. The best fit in this case was given by $k' = 3.78$, k'' = 2.39 x 10^{-36}, b = 12.7 and ΔE = 439 kJ/mol, which is almost double the previous value of ΔE though still not as high as 514 kJ/mol. The improved parity plot is shown as Figure 9 and the improved AAD is 28.6%.

CONCLUSIONS

1. Initial fouling rates, $\dot{R}_{fo}$, measured in transitional and turbulent flow as the observed linear fouling rate in the scale-resistance control period, followed the *qualitative* trends with surface temperature and velocity indicated by the Initial Fouling Rate Model, as derived for crystallization fouling with second order surface-integration kinetics. Significant *quantitative* deviations from the model were recorded. These were much reduced by introducing an additional adjustable parameter involving the deposition-fluid interface temperature T_s (assumed equal to $T_{w,c}$), rationalized as a crude method of accounting for the temperature effect on the nucleation that accompanies crystal growth.

2. Fouling activation energies, ΔE_f, showed almost a ten-fold increase with velocity from its lowest value of 66 kJ/mol at V = 0.1 m/s to its highest value of 514 kJ/mol at V = 1.6 m/s. This increase is explainable by the fact that surface attachment (or "surface integration" or "surface reaction"), which is strongly temperature dependent, gradually overtakes mass transfer, which is weakly temperature dependent, as the governing deposition mechanism as the velocity is increased. However, both the best-fit attachment activation energy ΔE of 263 kJ/mol generated by the original IFRM and the ΔE = 439 kJ/mol generated by the modified version fall short of the 514 kJ/mol, as required by the logic of the IFRM.

3. An attempt at isolating the surface integration kinetics of calcium sulphate crystallization in the bulk solution in a batch reactor gave values of the activation energy for the surface reaction about four times the values obtained by several other investigators in the literature (c.f. Fahiminia, 2007), but only one-third of the maximum value obtained for the fouling activation energy. It was tentatively concluded that crystallization in the bulk solution follows different kinetics than crystallization on a foreign surface.

ACKNOWLEDGMENTS

The authors are grateful to the Natural Sciences and Engineering Research Council of Canada for financial support.

NOMENCLATURE

A = pre-exponential factor, $m^2.K.kJ^{-1}$

A_c = crystal surface area, m^2

A_{co} = crystal surface area at time t_o, m^2

A_{c1} = crystal surface area at time t_1, m^2

a = coefficient lumped with k'' in modified IFRM

b = exponent on T_s in modification of IFRM, -

C = $CaSO_4$ concentration, $kg \cdot m^{-3}$

C_b = bulk concentration of $CaSO_4$, $kg \cdot m^{-3}$

C_{bo} = initial bulk concentration of $CaSO_4$, $kg \cdot m^{-3}$

C_{b1} = bulk concentration of $CaSO_4$ at time t_1, $kg \cdot m^{-3}$

C_s = $CaSO_4$ saturation concentration, $kg \cdot m^{-3}$

C_w = $CaSO_4$ concentration adjacent to wall, $kg \cdot m^{-3}$

ΔC = overall driving force, $C_b - C_s$, $kg \cdot m^{-3}$

D = molecular diffusivity of $CaSO_4$ in water, $m^2.s^{-1}$

d = inside tube diameter, m

ΔE = surface-integration activation energy, $J \cdot mol^{-1}$

ΔE_f = fouling activation energy, $J \cdot mol^{-1}$

f = Fanning friction factor, -

G = mass velocity of fouling solution, $kg \cdot m^{-2} \cdot s^{-1}$

k = lumped rate constant, $m^3 \cdot kg^{-1} \cdot s^{-1}$

k_a = surface attachment coefficient, $m^4 \cdot kg^{-1} \cdot s^{-1}$

k_m = mass transfer coefficient, $m \cdot s^{-1}$

k_r = conventional surface reaction rate constant for second order reaction rate, $m^4 \cdot kg^{-1}s^{-2}$

k' = constant in Equation (6), -

k'' = constant in Equation (7), $kg \cdot s^2 \cdot m^{-4}$

m = crystal mass at time t, kg

m_1 = crystal mass at time t_1, kg

n = Reaction Order, -

$\dot{q}$ = heat flux, $W \cdot m^{-2}$

R = universal gas constant, 0.008314 kJ/mol·K

R_f = fouling resistance, $m^2 \cdot K \cdot W^{-1}$

$\dot{R}_{fo}$ = initial fouling rate, $m^2 \cdot K \cdot J^{-1}$

Re = Reynolds number $= dG \cdot \mu^{-1}$,

Sc = Schmidt number $= \upsilon \cdot D^{-1}$, -

T = temperature, K

T_b = local bulk fluid temperature, ºC or K

T_s = surface temperature = clean inside wall or deposit-fluid interface temperature, K

T_w = inside wall temperature, K

$T_{w,c}$ = clean inside wall temperature, K

$T_{w,o}$ = outside wall temperature, K

t = time, s

t_o = time when first solute concentration is C_{bo}, s

t_1 = time when first solute concentration is measured after precipitation has started in crystal growth experiment, s

U = overall heat transfer coefficient, $W \cdot m^{-2} \cdot K^{-1}$

U_c = value of U when inside wall is clean, $W \cdot m^{-2} \cdot K^{-1}$

V = bulk fluid velocity, m/s

v_* = friction velocity $\equiv V\sqrt{f/2}$, $m \cdot s^{-1}$

x = vertical distance along heated fouling tube, m

Greek Symbols

α = coefficient in Eq. (13), $m^4 \cdot K \cdot s \cdot kg^{-1} \cdot J^{-1}$

β = coefficient in Eq. (13), $K \cdot s^{-2} \cdot kg^{-1} \cdot J^{-1}.m^7$

μ = dynamic viscosity, $kg \cdot m^{-1} \cdot s^{-1}$

λ_f = thermal conductivity of fouling deposit, $W \cdot m^{-2} \cdot K^{-1}$

υ = kinematic viscosity, $m^2 \cdot s^{-1}$

ρ_f = density of fouling deposit, $kg \cdot m^{-3}$

ϕ =deposition flux, $kg \cdot m^{-2} \cdot s^{-1}$

REFERENCES

Bansal, B. and H. Müller-Steinhagen, 1993, "Crystallization Fouling in Plate Heat Exchangers" *ASME Journal of Heat Transfer*, Vol. 115, pp. 584-591.

Bansal, B., Chen, X. D., Mueller-Steinhagen, H., 2005, "Deposition and Removal mechanisms during Calcium Sulphate Fouling in Heat Exchangers", *International Journal of Transport Phenomena* Vol. 7(1), pp. 1-22.

Bohnet, M., 1987, "Fouling of Heat Transfer Surfaces" *Chem. Eng. Technol.* Vol. 10, pp. 113-125.

Bohnet, M., W. Augustin and H. Hirsch, 1999, "Influence of Fouling Layer Shear Strength on Removal Behaviour" in "*Proc. Int. Conf. Understanding Heat Exchanger Fouling and Its Mitigation*", T.R. Bott, Ed., Il Ciocco Conf. Centre, Castelvecchio Pascoli, Italy, May 1997, begell house inc., New York, pp. 201-208.

Einstein, A., 1905, "Investigations on the Theory of Brownian Movement", Dover, New York, 1956 (English translation of paper that first appeared in *Ann. Phys.* Vol. 17, 549, Leipzig).

Epstein, N., 1994, "A Model of the Initial Chemical Reaction Fouling Rates for Flow within a Heated Tube, and its Verification", in "*Heat Transfer, Proc. 10th Int. Heat Transf. Conf.* Vol. 4," Brighton, UK (1994), pp. 225-229.

Fahiminia, F., 2007, "Initial Fouling Rate and Delay Time Studies of Aqueous Calcium Sulphate Scaling Under Sensible Heating Conditions", Ph.D. Thesis, The University of British Columbia.

Konak, A.R., 1974, "A New Model for Surface Reaction-Controlled Growth of Crystals from Solution," *Chem. Eng. Sci.* Vol. 29, pp. 1537-1543.

Krause, S., 1993, "Fouling of Heat Transfer Surfaces by Crystallization and Sedimentation," *International Chemical Engineering* Vol. 33, pp. 355-401.

Middis, J., H. Müller-Steinhagen, S.T. Paul and G.G. Duffy, 1998, "Reduction of Heat Transfer Fouling by the Addition of Wood Pulp Fibers," *Heat Transfer Engineering* Vol. 19, pp. 36-44.

Mori, H., M. Nakamura and S. Toyama, 1996, "Crystallization Fouling of Calcium Sulphate Dihydrate on Heat Transfer Surfaces," *J. Chem. Eng. Japan* Vol. 39, pp. 166-173.

Mwaba, M.G., C.C.M. Rindt, M.A.G. Vorstman and A.A. Van Steenhoven, 2001, "Calcium Sulphate Deposition and Removal Characteristics on a Heated Plate", in "*Proc. 4th Int. Conf. Heat Exchanger Fouling: Fundamental Approaches & Technical Solutions*," H. Müller-Steinhagen, M.R. Malayeri and A.P. Watkinson, Eds., Davos Switerland, July 2001, Publico Publications, Germany, pp. 57-63.

Najibi, S.H., H. Müller-Steinhagen and M. Jamalahmadi, 1997, "Calcium Sulphate Scale Formation During Subcooled Flow Boiling," *Chem. Eng. Sci.* Vol. 52, pp. 1265-1283

Nancollas, G.H., 1968, "Kinetics of Crystal Growth from Solution," *J. Crystal Growth* Vol. 3-4, pp. 335-339.

O'Rourke, J.D. and R.A. Johnson, 1955, "Kinetics and Mechanism in Formation of Slightly Soluble Ionic Precipitates," *Analytical Chemistry* Vol. 27, pp. 1699-1704.

Petukhov, B.S., 1970, "Advances in Heat Transfer", T.F. Irvine and J.P. Hartnett, Eds., Academic Press, New York.

Ritter, R.B., 1983, "Crystalline Fouling Studies," *Trans. ASME* Vol. 105, pp. 374-379.

Rose, I.C., A.P. Watkinson and N. Epstein, 2001, "Model Investigation of Initial Fouling Rates of Protein Solutions in Heat Transfer Equipment," in "*Proc. Int. Conf. Mitigation of Heat Exchanger Fouling and Its Economic and Environmental Implications*," T.R. Bott, A.P. Watkinson and C.B. Panchal, Eds., Banff, Alberta, Canada, July 1999, begell house inc., New York, pp. 223-229.

Rose, I. C., Watkinson, A.P., Epstein, N., 2000, "Testing a Mathematical Model for Initial Chemical Reaction Fouling using a Dilute Protein Solution," *Canadian Journal of Chemical Engineering* Vol. 78, pp. 5-11.

Smith, B.R. and F. Sweett, 1971, "The Crystallization of Calcium Sulphate Dihydrate," *J. Colloid & Interface Sci.* Vol. 37(3), pp. 612-618.

Vašák, F., B.D. Bowen, C.Y. Chen, F. Kastanek and N. Epstein, 1995, "Fine Particle Deposition in Laminar and Turbulent Flows," *Can. J. Chem. Eng.* Vol. 73, pp. 785-792.

Wilson, D.I., Watkinson, A. P., 1996, "A Study of Autoxidation Reaction Fouling in Heat Exchangers," *Canadian Journal of Chemical Engineering* Vol. 74, pp. 236-246.

Wilson, D.I., 1994, "Model Experiments of Autoxidation Reaction Fouling", Ph.D. Thesis, The University of British Columbia.